POPDC2 a novel susceptibility gene for conduction disorders

Susanne Rinné[a], Beatriz Ortiz-Bonnin[a], Birgit Stallmeyer[b], Aytug K. Kiper[a], Lisa Fortmüller[c,d], Roland F.R. Schindler[e], Ursula Herbort-Brand[e], Nashitha S. Kabir[f], Sven Dittmann[b], Corinna Friedrich[b,&], Sven Zumhagen[b], Francesca Gualandi[g], Rita Selvatici[g], Claudio Rapezzi[h], Eloisa Arbustini[i], Alessandra Ferlini[g,j], Larissa Fabritz[d,f,k], Eric Schulze-Bahr[§,b], Thomas Brand[§,e], and Niels Decher[a,§,*]

[a] Institute for Physiology and Pathophysiology, Vegetative Physiology, Philipps-University of Marburg, Marburg, Germany;
[b] Institute for Genetics of Heart Diseases (IfGH), University Hospital Münster, Münster, Germany;
[c] Institute of Human Genetics, Department of Genetic Epidemiology, University Hospital Münster, Münster, Germany;
[d] Cardiology II-Electrophysiology, University Hospital Münster, Münster, Germany;
[e] National Heart and Lung Institute, Imperial College London, London, United Kingdom;
[f] Institute of Cardiovascular Sciences, University of Birmingham, Birmingham, United Kingdom;
[g] Unit of Medical Genetics, Department of Medical Sciences, University of Ferrara, Ferrara, Italy;
[h] Unit of Cardiology, Policlinico S. Orsola Bologna, Italy;
[i] Policlinico S. Matteo, Pavia, Italy;
[j] Dubowitz Neuromuscular Centre, Developmental Neuroscience Programme, University College of London, Institute of Child Health, London, United Kingdom;
[k] Department of Cardiology, University Hospital Birmingham, Birmingham, United Kingdom

[&] currently at the Institute for Human Genetics, University Hospital Münster, Münster, Germany.

Running head: POPDC2 and atrioventricular block

Word count: 8103

[§] Shared senior authors

*Corresponding author:

Prof. Dr. Niels Decher,
Institut für Physiologie, Vegetative Physiologie,
Philipps-Universität Marburg,
Deutschhausstraße 1-2
35037 Marburg, Germany
E-Mail: decher@staff.uni-marburg.de
T: + 49-6421-28-62148
F: + 49-6421-28-66659

ABSTRACT

Despite recent progress in the understanding of cardiac ion channel function and its role in inherited forms of ventricular arrhythmias, the molecular basis of cardiac conduction disorders often remains unresolved. We aimed to elucidate the genetic background of familial atrioventricular block (AVB) using a whole exome sequencing (WES) approach. In monozygotic twins with a third-degree AVB and in another, unrelated family with first-degree AVB, we identified a heterozygous nonsense mutation in the *POPDC2* gene causing a premature stop at position 188 (POPDC2^{W188*}), deleting parts of its cAMP binding-domain. Popeye-domain containing (POPDC) proteins are predominantly expressed in the skeletal muscle and the heart, with particularly high expression of POPDC2 in the sinoatrial node of the mouse. We now show by quantitative PCR experiments that in the human heart the POPDC-modulated two-pore domain potassium (K_{2P}) channel TREK-1 is preferentially expressed in the atrioventricular node. Co-expression studies in *Xenopus* oocytes revealed that POPDC2^{W188*} causes a loss-of-function with impaired TREK-1 modulation. Consistent with the high expression level of POPDC2 in the murine sinoatrial node, POPDC2^{W188*} knock-in mice displayed stress-induced sinus bradycardia and pauses, a phenotype that was previously also reported for *POPDC2* and *TREK-1* knock-out mice. We propose that the POPDC2^{W188*} loss-of-function mutation contributes to AVB pathogenesis by an aberrant modulation of TREK-1, highlighting that *POPDC2* represents a novel arrhythmia gene for cardiac conduction disorders.

Keywords:

atrioventricular block

arrhythmia

ion channels

whole exome sequencing

1. Introduction

Disorders affecting the cardiac conduction system can induce serious and potentially life-threatening bradyarrhythmias. These dysfunctions can become evident by impaired cardiac conduction through the atrioventricular (AV) node, the His-bundle or the Purkinje system with right or left bundle branch block (RBBB or LBBB) and/or a broadening of the QRS complex. Hereditary forms of arrhythmias are predominantly caused by mutations in genes encoding ion channels or their modulating subunits. Mutations in the *SCN5A* gene encoding the cardiac sodium channel or its ß-subunits are associated with progressive cardiac conduction disorder (PCCD) [1-3] and with congenital sick sinus syndrome (SSS) [1,4]. In addition, mutations in the *TRPM4* channel gene cause autosomal-dominant hereditary forms of PCCD including AV conduction abnormalities [5]. Moreover, mutations in the *LMNA* gene may first present as AV conduction disorder and later as progressive heart failure and dilated cardiomyopathy [6]. Despite recent progress in the understanding of cardiac ion channel function and their role in inherited forms of ventricular arrhythmias, the genetic background of cardiac conduction disorders often remains unresolved.

The Popeye domain containing (*POPDC*) gene family encodes proteins with three transmembrane domains which are predominantly expressed in the heart and skeletal muscle [7,8]. The C-terminal parts of the proteins harbouring the highly conserved Popeye-domain which contains a cAMP binding site are localized to the cytoplasm [9]. POPDC proteins are known to interact with the two-pore domain potassium (K_{2P}) channel TREK-1 thereby enhancing its current amplitude [9]. We have previously reported that cAMP binds with high affinity to the Popeye domain, abolishing the current modulation of TREK-1 channels [9].

TREK-1 plays a major role in murine sinoatrial pacemaking as cardiac-specific ablation of TREK-1 in mice causes a bradycardia with episodes of sinus pauses following stress [10]. In the mouse heart, POPDC2 is expressed in atrial and ventricular myocytes [8], however a dominant expression in the sinoatrial and AV node and other parts of the cardiac conduction system was described [9]. Interestingly, in mice, *POPDC1* and *POPDC2* null mutants presented a comparable phenotype as the TREK-1 knock-out mice, with a strong stress-induced sinoatrial node dysfunction [9,10]. On the other hand, in *POPDC1/POPDC2* double knock-out mice also an AVB was prevalent [11], compatible with

3

observations from zebrafish in which morpholino oligonucleotide-mediated knock-down of *POPDC2* led to AVB [12]. In humans we recently identified a POPDC1^{S201F} mutation which causes AV block (AVB) and autosomal recessive limb-girdle muscular dystrophy (LGMDR25) [13]. Another three recessive mutations in *POPDC1* are associated with AVB and LGMD of variable severity and age at onset [14], while mutations in *POPDC3* are causing LGMD (LGMDR26) with no cardiac involvement [15].

To elucidate the genetic background of familial AVB we used a whole exome sequencing (WES) approach in a family with AVB and identified the heterozygous *POPDC2* nonsense variant *POPDC2*^{W188*}. The same POPDC2^{W188*} mutation was subsequently identified in another family with dominant inheritance. Mechanistically, our data suggest that the POPDC2^{W188*} mutation causes impaired AV conduction that is mediated by a dysregulation of TREK-1 potassium channels.

2. Materials and methods

2.1 Study population: Clinical and targeted DNA sequence analysis

In the present study we included patients with isolated atrioventricular block (AVB; $n = 22$), idiopathic sinus node dysfunction (SND; $n = 32$), right or left bundle branch block (RBBB, LBBB; $n = 13$), progressive cardiac conduction disease (PCCD; $n = 5$) and atrial fibrillation (AF; $n = 10$). We previously excluded mutations in *SCN5A* and *TRPM4* in patients with PCCD, RBBB, LBBB and AVB and mutations in *HCN4* in patients with SND. Stress electrocardiogram (ECG), Holter ECG and transthoracic echocardiogram were obtained from all mutation carriers and their relatives. Detailed clinical and family histories, including cardiac symptoms, pacemaker implantation, and standard 12-lead ECGs were obtained in our specialized outpatient clinic dedicated for inherited cardiovascular disorders.

Genomic DNA was isolated from venous blood samples, and the four exons of the *POPDC2* gene were amplified using primers located 60-100 bp from the exon-intron boundaries (primer sequences available upon request). Obtained DNA sequence information was compared with the *POPDC2* wild-type sequence (NM_022135.2), nucleotide variants of interest were confirmed in a second independent sequencing reaction on both strands. ECG analysis was performed mainly upon conventional 12-lead ECG recordings with standard lead positions (paper speed 25 or 50 mm/s). Recordings were digitalized by scanning in a high-resolution format and were imported into a graphic program (DatInf® Measure, Germany) for accurate measurements. Duration of the PQ, QRS and QT intervals as well as RR intervals for calculating the heart rate were measured in two consecutive beats and provided as mean values with standard deviation. ECG and arrhythmia analyses were independently performed by two cardiologists.

2.2 Whole exome sequencing (WES) in a family with AVB

A library preparation for WES was performed from blood samples according to Agilent's Sure Select Protocol Version 1.2. The concentration of the library was determined using Agilent's qPCR NGS

Library Quantification Kit and adjusted to a final concentration of 10 nM. Sequencing was performed on the Illumina HiSeq2000 platform using TruSeq v3 chemistry. FastQ files were mapped to the human genome (hg19/b37) using Burrows Wheeler Aligner (BWA) package (version 0.6.1). Local realignment of the mapped reads around potential insertion/deletion (indel) sites was carried out with the Genome Analysis Tool Kit (GATK) version 1.4. Duplicate reads were marked using Picard (version 1.62). Additional BAM file manipulations were performed with Samtools 0.1.18. Phred-scaled quality scores were recalibrated using GATK's covariance recalibration. SNP and indel variants were called using the GATK Unified Genotyper. Variants were annotated using Ensembl to show which genes and transcripts are affected. Obtained vcf files were filtered using the VariantStudio software (Illumina).

2.3 Nucleotide variant analysis and variant filtering after WES

First, variants causing potentially serious consequences, namely non-synonymous coding, splice site region, deletions, insertions or stop gained and stop lost, were selected from all high quality regions (coverage $\geq$ 20x and filter PASS). Next, common polymorphic variants (i.e., minor allele frequency (MAF) $\geq$ 1%) being listed in the database of the NHLBI GO Exome sequencing Project (ESP) (http://evs.gs.washington.edu/EVS/) were excluded since unlikely to cause a rare disease. The remaining nucleotide variants were filtered against 452 prioritized, cardiovascular genes relevant for cardiac function or inherited cardiovascular conditions (CARDIO gene panel [16], in-house database). Filtered variants hereafter were checked for their presence in the control population database of the Exome Aggregation Consortium (ExAC) (http://exac.broadinstitute.org) as well as the Human Genetic Variation Database (HGVD). Next, all variants annotated with a MAF $\geq$ 0.05% were excluded to filter only for uncommon and very rare variants. Finally, the predicted functional effect of amino acid change on regular protein function was predicted by PolyPhen2, SIFT, Mutation Taster, and PROVEAN for concordantly "deleterious/damaging" effects, whereas effects on splice site region variants was calculated by MaxEnt (http://genes.mit.edu), NNSPLICE http://www.fruitfly.org) and HSF (http://www.umd.be/HSF/). Since WES was finally performed in a total of three family members (proband 10031-1, unaffected father 10031-5 (father) and affected twin sibling 10031-4), we first

selected uncommon, rare variants (MAF ≤1% in EVS) with serious consequences from all high quality variants. Next, only shared variants that were present in all affected family members were taken into account if they were absent or very rare (MAF ≤0.05%) in control population databases (Exome Aggregation Consortium (ExAC), Japan Human Genetic Variation Database (HGVD)). Finally, variants also were filtered for cardiac expression (according to the data from MOPED [17] and PaxDb (http://pax-db.org)).

Analysis of variants in cardiac genes panel in the second family with AVB (GD1090, BL1091): among 394 (GD1090) and 411 (BL1091) variants identified in the 174 cardiac genes, non-synonymous coding, splice site region, deletions, insertions, stop gained or stop lost, were selected from all high quality variants (coverage ≥ 80x and filter PASS) common to both subjects. Next, all variants with a MAF ≥ 1% were excluded. Among the remaining variants, the effect of amino acid substitutions was predicted by bioinformatics tools as described above.

2.4 RNA extraction and RT-PCR

Total RNA was isolated from EDTA blood and fibroblasts obtained from skin biopsies of POPDC2^{W188*} mutation carriers using QIAamp RNA Blood Mini Kit (QIAGEN) according to the manufacturer's instructions. Single-stranded cDNAs were synthesized from 2 μg of RNA from each sample using a SuperScript First-Strand RT-PCR kit (Invitrogen Corporation) with random hexamers. In the subsequent PCR reaction, 2 μl of the cDNA product and POPDC2 forward primer: 5'-tctctggccgggttcgtgtgagc-3' (spanning exon 1-2) and reverse primer: 5'-ccagcagagccgagaagaggcagg-3' (located within exon 3) were used for PCR amplification of transcripts covering the critical interval with the predicted nonsense variant. The resulting PCR products (200 bp) were analyzed by electrophoresis in 2% agarose gels. The excised band was purified using a QIAEX Gel Extraction Kit (QIAGEN) and sequenced.

2.5 Quantitative PCR (qPCR)

To study the expression pattern of *POPDC2* and *KCNK2* (TREK-1) gene in human cardiac compartments, RNA from human atrium, sinoatrial node, AV node, and Purkinje fibers were used (Analytic Biological Service Inc., ABS). RNA was reverse transcribed into cDNA using Quanti Tect Reverse Transcription Kit (Qiagen). Quantitative RT-PCR was performed using a Rotor-Gene® (Qiagen), Rotor-Gene SYBR Green PCR Kit (Qiagen), primers (1.0 μM), and mentioned cDNA. The primers used for QPCR are: GAPDH for 5'-AGTCAACGGATTTGGTCGTAT-3', GAPDH rev 5'-ACCATGTAGTTGAGGTCAATGAAG-3'; POPDC2 for 5'-CAGGCCAGACAGTGGCATACTGG-3', POPDC2 rev 5'-TTAAAGTTCAGGCGTGTGGGTTGG-3'; TREK-1 for 5'-GAAGAGGTGGGAGAGTTCAGAG3', TREK-1 rev 5'-TACAAGGAGTCAGCTCCTGATTG-3'. All qPCR reactions were performed using 2 min at 50°C, 5 min initial activation step at 95 °C, followed by 45 cycles of 15 s at 95 °C, 30 s at 60 °C and 30 s at 72 °C. To normalize POPDC2 or TREK-1 expression to GAPDH and to the expression in human atrium, the comparative ΔΔCt method has been used.

2.6 Two-electrode voltage clamp (TEVC) recordings in oocytes

Oocytes were obtained from anesthetized *Xenopus laevis* frogs and incubated in an OR2 solution containing (in mM): NaCl 82.5, KCl 2, $MgCl_2$ 1, HEPES 5 (pH 7.5) substituted with 2 mg/ml collagenase II (Sigma) to remove residual connective tissue. Subsequently, oocytes were stored at 18 °C in ND96 solution containing (in mM): NaCl 96, KCl 2, $CaCl_2$ 1.8, $MgCl_2$ 1, HEPES 5 (pH 7.5) supplemented with 50 mg/l gentamycin, 274 mg/l sodium pyruvate and 88 mg/l theophylline; when indicated the storage solution lacked theophylline. cRNA was synthesized with mMESSAGE mMACHINE-Kit (Ambion). The quality of cRNA was tested using gel electrophoresis and cRNA was quantified with the NanoDrop 2000 UV-Vis spectrophotometer (Thermo Scientific). Oocytes were each injected with 50 nl of cRNA. All TEVC recordings were performed at room temperature (20 - 22 °C) with a TurboTEC 10CD (npi) amplifier and a Digidata 1200 Series (Axon Instruments) as A/D converter. Micropipettes were made from borosilicate glass capillaries GB 150TF-8P (Science Products)

and pulled with a DMZ-Universal Puller (Zeitz). Recording pipettes had a tip resistance of 0.5-1.5 MΩ when filled with 3 M KCl solution. Pump currents of oocytes injected with Na/K ATPase were recorded using a K^+ free solution containing (in mM): NaCl 96, $CaCl_2$ 1.8, $MgCl_2$ 1, HEPES 5, sucrose 10 and $BaCl_2$ 5, pH 7.4 (NaOH) for inhibition of K^+ channels. Subsequently 10 mM sucrose was replaced by KCl in the continuous presence of $BaCl_2$. Data were acquired with Clampex 10 (Molecular Devices) and analyzed with Clampfit 10 (Molecular Devices) and Origin 7 (OriginLab Corporation).

2.7 Patch clamp experiments of HL-1 cells

HL-1 cells were transfected as described above. Transfected cells were identified by co-transfection with pEGFP. APs were recorded in the whole-cell configuration under current-clamp conditions at room temperature (22°C). For patch clamp experiments, HL-1 cells were superfused with solution containing (in mM): 135 NaCl, 5 KCl, 1 $CaCl_2$, 1 $MgCl_2$, 0.33 NaH_2PO_4, 10 glucose, 2 Na-pyruvate and 5 HEPES (pH 7.4 with NaOH) as previously described [16]. Patch clamp experiments were performed in the whole-cell configuration using pipettes pulled from borosilicate glass capillaries. The pipettes had a tip resistance of 3.0 - 4.0 MΩ when filled with a solution containing (in mM): 60 KCl, 65 K-glutamate, 5 EGTA, 2 $MgCl_2$, 3 K_2ATP, 0.2 Na_2GTP, and 5 HEPES (pH 7.2 with KOH). Data acquisition and command potentials were controlled with a commercial software program (Patchmaster, HEKA) with a sweep time interval of 1 s and a sample rate of 200 kHz. Data analysis of APs was done using the Fitmaster software (HEKA). For each cell measured, the AP parameters were averaged by analyzing ten subsequent APs. To determine the AP frequency, the beats per minute (bpm) were visually analyzed. The average bpm was analyzed from four independent transfections and dishes with untransfected HL-1 cells.

2.8 Generation of the POPDC2^{W188*} knock-in mouse model

The *POPDC2^{tm2Tbd}* (*POPDC2^{W188*}*) knock-in mouse model was generated by gene targeting in embryonic stem (ES) cells as previously described [18]. Briefly, two fragments of 5.3 kB and 6 kB were PCR amplified using a bacterial artificial chromosome (BAC) containing the mouse *Popdc2* genomic region and subcloned as 5' and 3' homology arms, respectively, into the pDTA-Amp plasmid [19]. A selectable/counter selectable cassette was placed into exon 2 of *Popdc2* resulting in a deletion of the coding sequence for amino acids 184 to amino acid 188. Subsequently, the *POPDC2^{W188*}* mutation was introduced with the help of a double stranded oligonucleotide, which substituted the selectable/counter selectable cassette. An *EcoR*V-FRT-neo-FRT-*Kpn*I-*Hind*III cassette was inserted 300 bp downstream of exon 2 that contains the *POPDC2^{W188*}* mutation (*Figure* 4). The targeting construct was verified by sequencing. Gene targeting was performed by electroporation of the *Asc*I linearized targeting vector into the B4 (C57BL/6J) ES cell line. Genomic DNA of G418-resistant clones were subjected to Southern blot analysis using 5'- and 3'-homology arm-specific DNA probes. 14 positive clones were expanded and re-examined by Southern blot analysis. Four of the re-confirmed clones were sequenced to verify the presence of the FRT sites and the point mutation. All four clones were injected into mouse blastocysts. Only one clone produced 9 high-percentage chimeras. Three male chimeras gave germ line transmission.

2.9 Mouse ECG recordings

To assess heart rate during stress, non-invasive ECGs were recorded from conscious young adult mice during gentle restrain by a tunnel system (ecgTunnel, EMKA Technologies, Paris, France) and beta-adrenergic stimulation (isoprenaline 2mg/kg i.p.). Heart rate analysis was performed with EMKA software (EMKA Technologies, Paris, France) summarized over a 5 min period. ECG recordings were screened manually for pauses. Here cycle length of 1.5 time of the previous, or in other words 50% or

more increase in cycle length compared to the previous cycle length, was regarded as a pause. Animal housing staff, staff performing and analyzing experiments were blinded to mouse genotype.

2.10 Methods used for euthanasia

We did not use euthanasia for mouse ECG recordings as these were *in vivo* experiments. For all other cases, e.g. generation, backcrossing and breeding of the POPDC2^{W188*} knock-in mouse line, the mice were killed/euthanized by a schedule 1 method under deep anaesthesia by isoflurane 5% inhalation. No frogs were killed in the course of this study as oocytes were surgically removed from female *Xenopus laevis* toads.

2.11 Statistical analyses

All values are expressed as means $\pm$ SEM. Error bars in all figures represent SEM values. *, $p > 0.05$; **, $p > 0.01$; ***, $p < 0.001$. Experiments in heterologous expression systems and QPCR experiments were analyzed statistically using unpaired Student´s t-test. Heart rates were compared by ANOVA using GraphPad Prism 7.01. Differences in occurrence of clusters of pauses were tested using Fisher's exact test.

2.12 Ethical approval

The study was in accordance with the ethical standards of the Declaration of Helsinki in its latest, revised version and with recommendations given by the local ethics committee of the University of Münster and the UNIFE local ethical committee. Written informed consent was given by all probands and their relatives prior to inclusion in the study. Experiments using *Xenopus* toads were approved by the local ethics commission of the "Regierungspräsidium Giessen". The POPDC2^{W188*} mouse work was approved by the Animal Welfare and Ethical Review Board of Imperial College London and licensed by the United Kingdom Home Office (PPL P2960EB2F and PPL PFDAAF77F).

3. Results

3.1 Whole Exome Sequencing (WES) identified a POPDC2 gene mutation in a twin pair with high degree atrioventricular block (AVB)

A 7-years old boy (proband 10031-1) presented with severe AVB (varying between 2nd to 3rd degree) (Fig. 1A and B) and due to symptoms (fainting and dizziness) he subsequently received a pacemaker. An identical clinical and symptomatic phenotype was seen for his monozygotic twin brother (10031-4) (Fig. 1A and B and Supplemental Fig. 1) who also received a pacemaker implant at the age of 10 years. Both twins had no evidence for a structural heart disease (as assessed by transthoracic echocardiography) and other ECG parameters, e.g., P-wave duration and morphology or QRS duration, were normal. In addition to the high degree AVB, both patients had ventricular premature beats (VPBs) originating during exercise from the right-ventricular outflow tract (RVOT; left bundle branch block (LBBB) with inferior axis). The relative amount was 1.7 – 1.9% of all ventricular beats per day. During exercise the ECG showed intrinsic sinus rhythm with consecutive ventricular stimulation without the need for pacing.

In the mother (10031-2), all cardiac examinations (ECG parameters, transthoracic echocardiography) and the personal history were so far unremarkable, without any pathology (Supplemental Table 1). The father (10031-3) had multiple VPBs (Supplemental Fig. 2) that were monomorphic and originating from the right-ventricular outflow tract (RVOT; LBBB with inferior axis). There was a normal AV conduction (188 ms), but at rest a slightly prolonged QRS duration (116 ms), in the absence of a structural heart disease.

In the third son (10031-5), ECG parameters were completely normal at rest, but there were exercise-related VPBs of the RVOT origin, as seen in his two twin brothers and father (Supplemental Table 1). There was no evidence for a structural heart disease or a cardiac conduction disorder. In summary, the two twin brothers had severe, early-onset and high-degree AVB; in addition, all male family members (father and three sons) had VPBs originating from the RVOT.

To identify the genetic background of severe AVB in the monozygotic twins, WES was initially performed in the proband 10031-1 (Fig. 1C). 35,433 high quality nucleotide variants in 12,942 genes were identified. Using a prioritization scheme as previously described [16], i.e. discarding common variants (minor allele frequency (MAF) >1%) reported in the NHLBI Exome Sequencing Project (ESP) and focusing on nucleotide variants causing serious consequences on the deduced protein sequence, 839 variants (2.5% of all) in 723 genes (5.7% of all) remained. These variants were further filtered using a panel of genes with a demonstrated cardiac expression or function (CARDIO gene panel [16]). None of the filtered 33 variants (in 26 genes) was listed as a disease causing mutation in the public version of the Human Genome Mutation Database (HGMD; http://www.hgmd.cf.ac.uk). After excluding amino acid variants that were also present in the control population database of the Exome Aggregation Consortium (ExAC) and the Japan Human Genetic Variation Database (HGVD) with a MAF <0.05%, only six variants remained (= 0.67% of selected variants): four non-synonymous amino acid exchanges, one stop-gained amino acid alteration and one splice region variant (Supplemental Table 2). These variants were analyzed by *in-silico* pathogenicity predictions, using up to five different pathogenicity prediction tools (PPTs).

Here, a concordant benign effect was predicted for the splice region variant (*ITPR3* gene, NM_002224.3), since no disruption of the acceptor site was calculated (by splice site predicting programs MaxEnt, NNSPLICE and HSF). Since the PPTs gave discordant results for the non-synonymous variants in *KCNF1* (NM_002236.4) and *SCNN1A* (NM_001159576.1), both were considered as variants of uncertain significance (VUS) and not further considered as disease-causing. Concordant harmful (pathogenic) effects were predicted for three gene variants. A non-synonymous SNP was identified in the cardiac isoform (N2-B/NM_003319.4) of the *TTN* gene, resulting in a p.Arg22177His exchange. *TTN* encodes the giant protein titin which is a component of the sarcomere and determines the sarcomeric viscoelasticity. The substituted arginine is located in the highly conserved A-band region of titin and present in cardiac and skeletal muscle isoforms. Mutations in *TTN* are typically associated with dilated and other cardiomyopathy forms (DCM, MIM:604145). The other variant with a concordant harmful prediction was located in *FKTN*, encoding fukutin, a protein related to the glycosylation of alpha-dystroglycan, which is associated with muscular dystrophy and DCM

13

(MIM:611615). As the brother (10031-5) had no AVB phenotype, but was sharing both rare variants in *FKTN* and *TTN*, it is unlikely that these variants primarily account for the AVB observed in the monozygotic twins. Finally, WES identified a heterozygous nucleotide variant (c.563G>A) in the *POPDC2* gene, introducing a premature stop codon at amino acid position 188 (p.Trp188*; POPDC2[W188*]) (Fig. 1C-E). This POPDC2[W188*] variant is very rare and only present once in 13,005 alleles (MAF: 0.0077%; Exome Variant Server (EVS)) and is predicted to truncate the POPDC2 protein in the Popeye-domain, directly in the proposed cAMP binding-domain [9] (Fig. 1E). Given the cardiac arrhythmia phenotypes of the *POPDC1/POPDC2* knock-out mice [9,11] and *POPDC2* deficient morphants in zebrafish [12] the POPDC2[W188*] variant was considered as the most likely candidate responsible for the AVB phenotype in our patients.
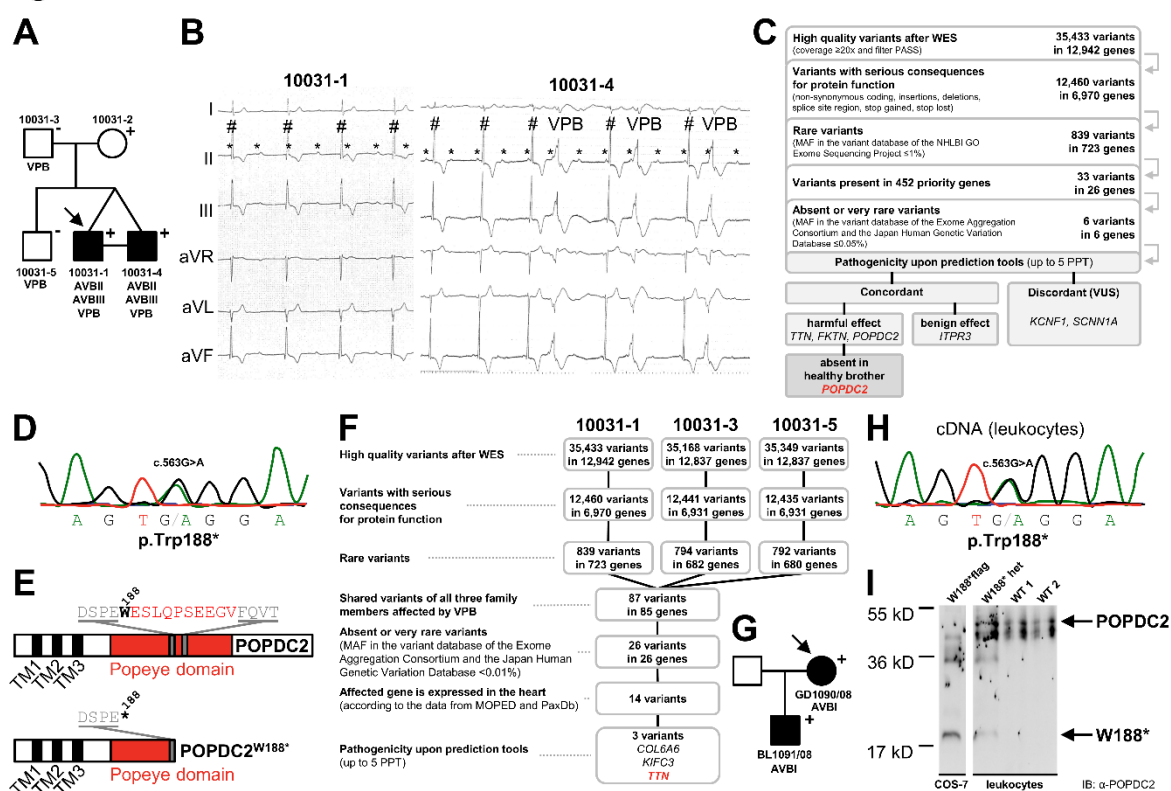
Figure 1

Fig. 1. Identification of a non-synonymous *POPDC2* gene variation (*POPDC2[W188*]*) in patients with AV block. (A) Pedigree of family 10031 with the heterozygous non-sense mutation p.Trp188*, (shortly: POPDC2[W188*]), as a result of the nucleotide variant (c.563G>A). Male are indicated by squares and female by circles. +, presence of POPDC2[W188*]; -, absence of POPDC2[W188*]. Solid symbols denote patients with AV block (AVB) II° or III°. Family members with ventricular premature beats (VPB) are indicated below. The propositus is indicated by an arrow. (B) ECG recordings of POPDC2[W188*] mutation carriers 10031-1 and 10031-4. *, P wave; #, QRS complex; VPB, ventricular premature beat with a superior axis. (C) Variant filtering strategy following whole exome sequencing of the propositus (10031-1). (D) Electropherogram illustrating the heterozygous c.563G>A (POPDC2[W188*]) mutation in the

14

POPDC2 genomic DNA of proband 10031-1 with severe congenital AVB. (E) Molecular architecture of POPDC proteins with three transmembrane domains and the intracellular Popeye domain (red), responsible for cAMP binding. Motifs that might be involved in cAMP binding are indicated in gray. The molecular architecture of the truncated POPDC2^{W188*} protein is depicted at the bottom. (F) Shared variant analysis of family members 10031-1, 10031-3 and 10031-5 affected by VPBs. (G) Pedigree of an independent family with the same heterozygous mutation p.Trp188* (c.563G>A) and AVB in 1st degree. Solid symbols denote *POPDC2^{W188*}* mutation carriers with AVB. (H) Electropherogram of *POPDC2* cDNA from leukocytes of proband 10031-1 demonstrates the expression of WT and *POPDC2^{W188*}* mutant allele. (I) Western Blot analysis using a POPDC2 specific antibody in leukocyte lysates of a mutation carrier (W188* het (10031-2)) or of non-mutation carriers (WT 1 (10031-3) and WT 2 (independent, healthy donor)). As a control protein lysates of COS-7 cells transfected with a POPDC2^{W188*} flag construct (W188*flag) was used. The calculated molecular weight of POPDC2 protein is about (40 kDa), whereas the truncated POPDC2^{W188*} protein is about 20 kDa.

To exclude that the AVB seen in the affected monozygotic twins is due to a *de novo* variant or a variant inherited in an autosomal recessive or X-chromosomal manner, we performed WES of the other family members and utilized family based filtering approaches (Supplemental Fig. 3). However, these analyses did not point towards any other genetic origin of the AVBs, highlighting the putative disease-causing relevance of the identified POPDC2^{W188*} variant.

Analyzing the ECG phenotypes in the family apart from high-degree AVB, we noted VPBs in the ECG recordings which were present in the siblings with AVB (10031-1, 10031-4) (Fig. 1B and Supplemental Fig. 1), but also in the healthy brother (10031-5) and father (10031-3) (Supplemental Fig. 2). To identify the molecular reason for the presence of VPBs in the four male family members, we performed a shared variant analyses of the family members with VPBs (Fig. 1F). Here we identified three non-synonymous amino acid variants in three different genes, namely *COL6A6*, *KIFC3* and *TTN* (Fig. 1F and Supplemental Table 3). Of note, the POPDC2^{W188*} variant was absent in the healthy brother (10031-5) and the father (10031-3), but present in the mother (10031-2) who was apparently asymptomatic (Fig. 1A). This observation might be related to a low penetrance of the *POPDC2^{W188*}* allele or due to sex-specific effects. Alternatively, a second genetic variant might have enhanced the potential pathogenicity of the *POPDC2^{W188*}* variant. Here, the non-synonymous *TTN* variant (p.Arg22177His) being present in all male family members, might enhance the AVB in the twins, in contrast to the mother without the *TTN* gene variant, since mutations in this gene have been previously associated with cardiac conduction disease in patients with arrhythmogenic right ventricular cardiomyopathy [20,21]. Thus, the observed VPBs might be related to an early-onset and arrhythmogenic stage of a DCM, since all family members did not have evidence for a structural heart

disease. Consistently, the *TTN* variant is present in the monozygotic twins harboring the POPDC2^{W188*} mutation, but not in the so far asymptomatic mother.

3.2 A candidate gene approach identifies another case of heterozygous POPDC2^{W188*} mutations associated with AVB

Next we used a candidate gene approach to probe whether other familial cases of AVB can be attributed to *POPDC2* mutations. Strikingly, following a screening of 82 patients with different arrhythmias (see Materials and methods section), we found the identical heterozygous *POPDC2^{W188*}* mutation in a mother and son affected by a 1st degree AVB (Fig. 1G). Thus, highlighting that the *POPDC2^{W188*}* variant might be associated with AV conduction disturbances in an autosomal dominant fashion, similar as in the other family we described above. Moreover, a panel of 174 genes with known association to inherited cardiac condition disorders was genotyped in the mother and son, while none of these genes were affected. Interestingly, both patients also had a variant in *MYH7* (p.E1801K), a mutation that was previously described in familial hypertrophic and dilated cardiomyopathies, associated with distal myopathy [22]. The *MYH7* variant might explain the mildly increased CK levels observed in the two AVB patients. On the other hand high CK levels were also reported in patients carrying biallelic *POPDC1* and *POPDC3* mutations, which in these cases were probably caused by an increased membrane permeability of the patient's skeletal muscle [13]. Interestingly, one of the patients carrying the *POPDC1^{S201F}* variant also displayed membrane discontinuities [13]. In conclusion, while the patients carrying the *POPDC2^{W188*}* allele do not display any overt skeletal muscle pathology, high CK levels may be caused either by a POPDC2-related subclinical membrane permeability not resulting in any clinical consequences or by the concomitant *MYH7* variation. *MYH7* mutations (OMIM #160760) are known to be associated with a wide clinical spectrum including asymptomatic hyperCKemia, scapulo-peroneal myopathy and proximal and distal myopathy with muscle hypertrophy [23]. It is also worth noting that *MYH7* has been recently proposed as a candidate gene for Brugada syndrome [24], a pure arrhythmogenic disorder. In our family the *MYH7* mutation could lead to high CK only or may lead to a very mild, later onset myopathy, as possibly suggested by the elevated CK level (357 U/L) in the

16

affected son. It could also be hypothesized that the coinheritance of *POPDC2* and *MYH7* mutations may influence the clinical picture or the disease severity, similarly to the other family described above (*POPDC2* and *TTN*) and according to the new concept of mutation load [25]. The two patients were paced and at the last clinical check two years ago they were both fine with still no extra-cardiac symptoms.

3.3 Detection of POPDC2^{W188*} RNA and protein in the patients' leukocytes

To investigate if the mRNA generated from the *POPDC2^{W188*}* allele is a target for nonsense mediated decay (NMD), we isolated total RNA from leukocytes of the two heterozygous *POPDC2^{W188*}* mutation carriers of the first family and performed RT-PCR amplification of exon 2 and subsequently a sequence analysis of the amplified DNA fragments. The *POPDC2^{W188*}* variant was detected in cDNA fragments obtained from both mutation carriers, indicating that the *POPDC2^{W188*}* allele is transcribed and stable, at least in leukocytes (Fig. 1H and I), and not subjected to NMD. In addition, using Western Blot analysis of the patients' leukocytes, we were able to detect the POPDC2^{W188*} truncated variant (Fig. 1I), indicating that also the protein is stably expressed in the patients.

3.4 POPDC2 and TREK-1 (KCNK2) are predominantly expressed in the human AV node and cardiac conduction system

Since POPDC proteins modulate the TREK-1 current amplitude [9] and POPDC2 is expressed in the cardiac conduction system of the mouse, we analyzed the expression profiles of TREK-1 (*KCNK2*) and POPDC2 within different regions of the human heart, using quantitative PCR experiments (Fig. 2A). Here, a very strong and predominant expression of TREK-1 was observed in the AV node (Fig. 2A). Also the POPDC2 expression was more prominent in the cardiac conduction system including the sinoatrial node, AV node and Purkinje fibres (Fig. 2A). This expression profile might be the basis for a TREK-1 modulation via POPDC2 especially in the human AV node.
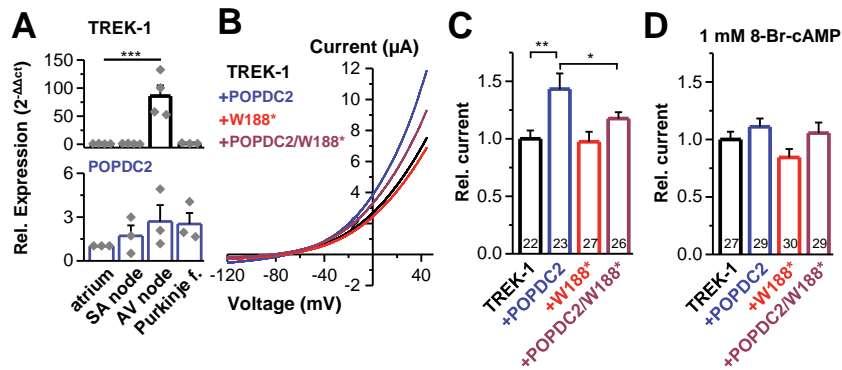
Figure 2

Fig. 2. Modulation of TREK-1 by wild-type POPDC2 and mutant POPDC2^{W188*}. (A) QPCR experiments determined the relative expression of human TREK-1 (upper panel) or POPDC2 (lower panel) relative to *GAPDH*, normalized to the atrial expression level. The relative expression was calculated by dividing means of ΔCt-values of each sample by mean ΔCt of atrium and setting into 2$^{-ΔΔCt}$. The experiments were performed as triplicates and averaged from three to four repeats. SA node, sinoatrial node; AV node, atrioventricular node; f., fibers. Statistical significance is indicated compared to atrial expression. (B) TREK-1 cRNA (0.25 ng) was injected alone or co-injected with POPDC2 (0.25 ng), mutant POPDC2^{W188*} (0.25 ng) or POPDC2 plus POPDC2^{W188*} (0.125 ng each, mimicking the heterozygous state) in *Xenopus laevis* oocytes which were subsequently stored in a solution lacking theophylline. Current voltage relationship was measured 48 h after injection. (C) Mean relative current amplitude at +40 mV normalized to TREK-1. (D) Experiments with similar amounts of cRNA as in (B-C), but oocytes were incubated in storage solution containing 8-Br-cAMP. After 48 h voltage-clamp recordings were performed as in (B). Number of experiments are indicated in parenthesis. Data are presented as mean ± SEM. Experiments were analyzed statistically using unpaired Student´s t-test. *, indicates p>0.05; **, p>0.01; ***, p<0.001.

3.5 Loss of TREK-1 current enhancement by POPDC2^{W188*}

To probe for potential changes in the TREK-1 modulation by mutant POPDC2^{W188*}, *Xenopus laevis* oocytes were injected with cRNA for TREK-1 alone, together with POPDC2 or POPDC2^{W188*} (Fig. 2B and C). While POPDC2 significantly enhanced TREK-1 current amplitudes, POPDC2^{W188*} did not alter TREK-1 currents (Fig. 2B and C). Co-expressing TREK-1 with a 1:1 mixture of POPDC2 and POPDC2^{W188*}, to mimic the heterozygous state identified in the patients, revealed again a loss of TREK-1 regulation (Fig. 2B and C). We have previously shown that the TREK-1 modulation by POPDC proteins is cAMP-dependent [9]. As expected, the TREK-1 current increase mediated by POPDC2 was abolished in the presence of 1 mM 8-Br-cAMP (Fig. 2D) [9]. This effect was observed for the TREK-1 channel expressed alone, together with wild-type POPDC2, mutant POPDC2^{W188*} alone or a `heterozygous´ mixture of POPDC2/POPDC2^{W188*} (which mimics the situation in the patients) (Fig. 2D). Similar results were obtained using theophylline containing storage solutions (data not shown). In

summary, POPDC2[W188*] and POPDC2/POPDC2[W188*] both have a reduced efficiency to increase TREK-1 current amplitudes, an effect that is likely to depolarize cells in the human AV node in a cAMP-dependent manner.

3.6 POPDC2[W188] depolarizes the membrane potential, slows the action potential (AP) frequency and reduces the upstroke velocity in spontaneously beating HL-1 cells*

HL-1 cells are spontaneously beating immortalized murine atrial cardiomyocytes, which resemble to some extent sinoatrial node myocytes [26]. They are able to continuously divide and spontaneously contract, while maintaining a differentiated cardiac phenotype [26]. POPDC2 and TREK-1 are expressed in the murine conduction system and the human AV nodal regions. As HL-1 cardiomyocytes resemble in their electrophysiological properties SA and/or AV nodal cells and also express TREK-1, we performed additional experiments using heterologous expression of the POPDC2[W188*] mutant in this cell type. Here the transfection of mutant POPDC2[W188*] reduces the AP frequency (Fig. 3A).
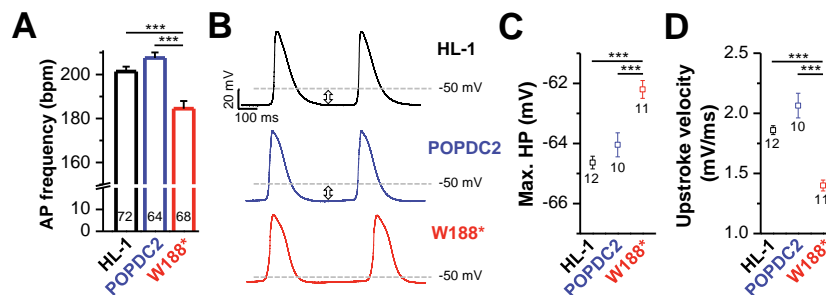
Figure 3

Fig. 3. POPDC2[W188*] slows the action potential frequency, depolarizes the maximal diastolic membrane potential and slows conductivity of spontaneously beating HL-1 cells. (A) AP frequency observed in non-transfected HL-1 cells or cells transfected with POPDC2 or POPDC2[W188*]. The numbers of cells analyzed are illustrated in the bars. (B) AP measurements in non-transfected HL-1 cells or cells transfected with either POPDC2 (blue) or POPDC2[W188*] (red) using whole cell current clamp recordings. (C) The maximal diastolic hyperpolarization (Max. HP) or (D) the upstroke velocity of the AP was plotted for non-transfected HL-1 cells or HL-1 cells transfected with POPDC2 or POPDC2[W188*]. Numbers of experiments are indicated. Data are presented as mean ± SEM. Experiments were analyzed statistically using unpaired Student´s t-test. ***, indicates $p<0.001$.

In addition, patch clamp experiments showed that the overexpression of POPDC2[W188*] (Fig. 3B) leads to a significant depolarization of the maximal diastolic membrane potential and a slowing of the upstroke

velocity (Fig. 3C and D), data that may explain a slowing of atrioventricular conduction caused by the POPDC2^{W188*} mutation.

3.7 Stress-induced sinus bradycardia and pauses in transgenic POPDC2^{W188*} mice

Given that in both families carrying the *POPDC2^{W188*}* mutation, the presence of additional gene variants might contribute to the pathogenesis of the AVB, we investigated whether the *POPDC2^{W188*}* mutation is the primary cause for the conduction disorders, by generating a *POPDC2^{W188*}* knock-in mouse model using a gene targeting approach in embryonic stem cells (Fig. 4).
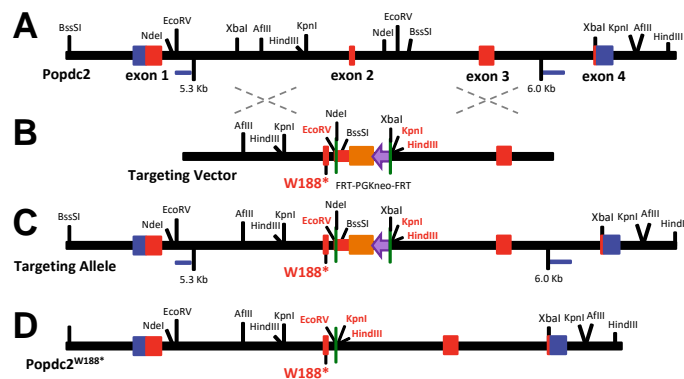
Figure 4

Fig. 4. Targeting strategy to produce the *POPDC2^{W188*}* mutant by homologous recombination in embryonic stem cells. (A) Wild-type *POPDC2* allele, (B) targeting vector to introduce the *POPDC2^{W188*}* mutant allele, (C) the targeted allele carrying the *POPDC2^{W188*}* mutation and (D) the *POPDC2^{W188*}* allele after removal of the neomycine cassette.

Strikingly, under sympathetic stimulation with isoprenaline, the homozygous *POPDC2^{W188*}* knock-in mice displayed relative sinus bradycardia compared to wild-type (Fig. 5A and B) with unaltered PR interval, P duration and QTc interval (Fig. 5C-E). In addition, we observed stress-induced pauses (Fig. 5F) in *POPDC2^{W188*}* knock-in mice, a phenotype that strongly resembles that of the *POPDC2* or *KCNK2 (TREK-1)* knock-out mice [9,10]. Fig. 5G and H illustrate representative examples of the heart rate monitored for wild-type and homozygous *POPDC2^{W188*}* mice. Note the constant heart rate of wild-type mice (Fig. 5G) in comparison to the variability in heart rate and the pauses occurring in *POPDC2^{W188*}* mice (Fig. 5H). Eleven out of twenty-eight transgenic *POPDC2^{W188*}* mice showed clusters of more than ten pauses or other arrhythmic events during restrained conscious ECG recordings,

while similar arrhythmias were only observed in two out of thirty wild-type mice (Fig. 5I). Strikingly, the reduction of heart rate in *POPDC2^{W188*}* mice was also present for the mutant knock-in animals that did not show arrhythmic events (Fig. 5J).
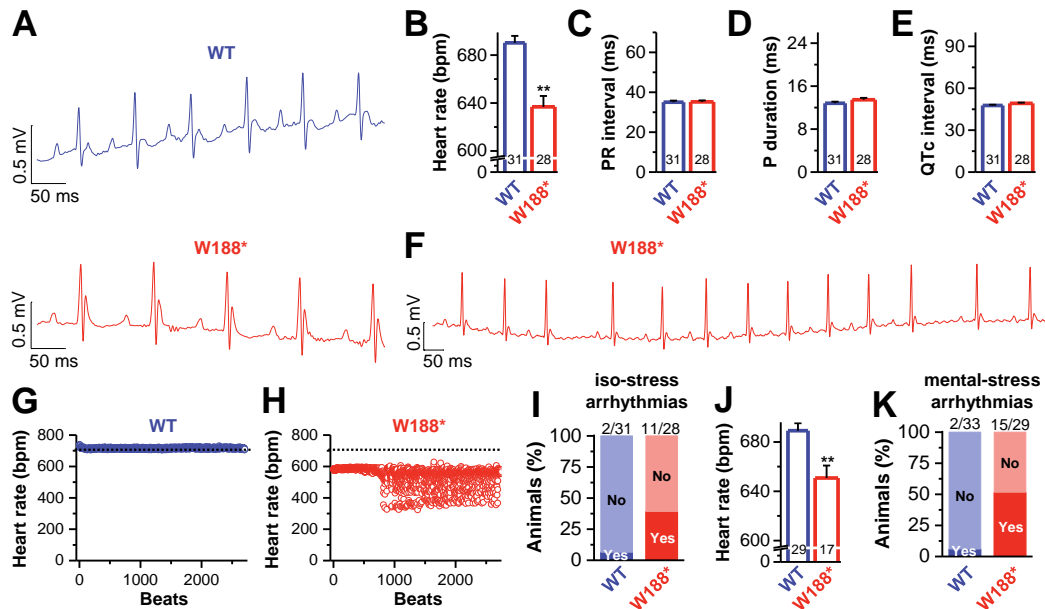
Figure 5

Fig. 5. Stress-induced relative sinus bradycardia and pauses in homozygous *POPDC2^{W188*}* mice. (A) Representative noninvasive ECG recordings under sympathetic stimulation with isoprenaline of conscious wild-type and transgenic *POPDC2^{W188*}* mice. (B) Analyses of the respective mean heart rate, (C) PR interval, (D) P-wave duration and (E) QTc interval. (F) Representative noninvasive ECG recording of *POPDC2^{W188*}* mice with sinoatrial arrhythmias. (G) Summary graph of heart rates of consecutive heart beats in wild-type and, (H) *POPDC2^{W188*}* mice. (I) Analyses of arrhythmias in wild-type and *POPDC2^{W188*}* animals under isoprenaline administration. (J) Analyses of the heart rate of the animals that did not show arrhythmic events. (K) Analyses of arrhythmias in wild-type and *POPDC2^{W188*}* mice which were under mental stress due to the handling for the ECG recordings. Numbers of experiments are indicated. Data are presented as mean ± s.e.m.. Heart rates and ECG intervals were compared by ANOVA using GraphPad Prism 7.01. Differences in occurrence of clusters of pauses were tested using Fisher's exact test. *, indicates $p > 0.05$; **, $p > 0.01$; ***, $p < 0.001$.

Moreover, *POPDC2^{W188*}* mice displayed highly similar sinus bradycardia and arrhythmias or AVB under the stress caused by the handling of the animals during non-invasive conscious ECG recordings (Fig. 5K and Supplemental Fig. 4). Here, fifteen out of twenty-nine transgenic *POPDC2^{W188*}* mice showed arrhythmias during restrained conscious ECG recordings, while similar pauses were only observed in two out of thirty-two wild-type mice (Fig. 5K).

Thus, we propose that *POPDC2* loss-of-function mutations cause SA node dysfunction in mice and contribute to AV node dysfunction in humans, mediated at least in part by a dysregulation of cardiac TREK-1 channels.

4. Discussion

The genetic basis for congenital disorders affecting pacemaking or AV conduction often remains elusive. To identify novel genes responsible for inherited forms of AVB we performed WES in a family with severe AVB and identified the $POPDC2^{W188*}$ mutation. POPDC proteins were recently identified as novel cAMP binding proteins involved in cardiac pacemaking and *POPDC1* or *POPDC2* null mutations in the mouse [9], as well as *POPDC2* morphants in zebrafish [12] suffered from severe cardiac arrhythmias. While in the *POPDC2* knock-out mouse a stress-induced sinoatrial node dysfunction was present [9], the *POPDC2* morphant zebrafish and *POPDC1/POPDC2* double knock-out mice displayed sinoatrial node dysfunction but also AVB [11]. In the context of conduction disorders, *POPDC1* was recently associated with changes in QRS duration in a genome-wide association study [27]. Moreover, several *POPDC1* missense mutations are causing AVB and autosomal recessive limb-girdle muscular dystrophy (LGMDR25) [13,14], which indicates that POPDC proteins may, in addition to affecting sinoatrial nodal pacemaking, also play a key role for AV conduction.

Still the mechanism how POPDC proteins affect the cardiac conduction system remains to a large part unexplained and the only cardiac ion channel that currently is known to be modulated by POPDC isoforms is the K_{2P} channel TREK-1 [9,13]. Strikingly, TREK-1 was recently described to play a major role in controlling the excitability of the murine sinoatrial node [10]. While the role of TREK-1 in human cardiac pacemaking has not yet been carefully studied, the preferential expression of TREK-1 in the human AV node, as we have observed here, is in line with the conduction disorder present in our patients.

The reduction of the TREK-1 currents by the $POPDC2^{W188*}$ mutation should depolarize the membrane potential in cells of the AV node (humans) and/or the SA node (mice) where TREK-1 appears to be preferentially expressed. Our *in vitro* experiments in HL-1 pacemaker-like cells support that the $POPDC2^{W188*}$ mutation can cause AVB by such or a similar mechanism, since in these cells the $POPDC2^{W188*}$ mutation causes a mild depolarization with a slowing of the upstroke velocity and reduced spontaneous AP frequency. Accordingly, minor changes in the membrane potential or upstroke velocity, as we have observed here might result in a reduced efficiency of the excitation to exit the human AV node.

TREK-1 is the only ion channel that is described to be modulated by POPDC2 so far. The pacemaker current (I_f) was not altered in *POPDC1* or *-2* deficient mice and additionally the current amplitudes of the K$_{2P}$ channel TASK-1 was not modulated by POPDC in co-expression studies [9]. POPDC proteins were reported to interact with several proteins, including zonula occludens 1 protein (ZO-1), atypical protein kinase C (aPKC), dystrophin, dysferlin, guanine nucleotide exchange factor T (GEFT), vesicle-associated membrane proteins (Vamp2 and 3), N-myc downregulated gene family member 4 (NDRG4), LRP6, PR61α, c-Myc or caveolin-3. Since these interaction partners are non-electrogenic and thus not directly involved in cellular electrophysiology, the contribution to the observed phenotypes in HL-1 cells or the *POPDC2*^{W188*} mice appears to be minor. However, we cannot rule out that POPDC2 is also interacting with other ion channels and that a dysregulation of those by POPDC2^{W188*} might contribute to the observed phenotype.

Since our genetic data point towards a role of the *POPDC2*^{W188*} mutant as a risk factor for conduction disorders in humans, we chose a homozygous mouse model to proof, that the *POPDC2*^{W188*} mutation confers an arrhythmic potential to our patients. We have chosen to study homozygous instead of heterozygous mice, as transferring data from mice to man (animal models) is in general limited and given the variability in mouse models, it is a commonly used approach to probe homozygous transgenic animals in order to 'not lose' a phenotype. Strikingly however, examining the *POPDC2*^{W188*} loss-of-function mutation in mice, we observed a highly comparable phenotype with sinus bradycardia and stress induced pauses, as described for the complete loss of the *POPDC2* gene in the respective knock-out mice [9].This data, of course, is not suitable to prove a monogenetic dominant-negative inheritance trait, but clearly provides evidence that the POPDC2^{W188*} mutant provides a risk for sino-atrial arrhythmias in mice and given the preferential expression of TREK-1 in the human AV node, we think that that this risk of the *POPDC2* loss-of-function mutant allele is most likely conferred to humans in the form of AV conduction disorders.

Although the sinus bradycardia observed in *POPDC2*^{W188*} knock-in mice does not fully mirror the phenotype of our patients, it nonetheless strongly supports the concept that the *POPDC2*^{W188*} variant is a disease-causing loss-of-function mutation that is able to induce cardiac conduction disorders. Most importantly, the different cardiac pathologies observed in mice versus humans is most likely related to

species-dependent differences in the expression profile of TREK-1 or other ion channels involved. Strikingly, TREK-1 seems to play a major role in murine sinoatrial pacemaking [10] while our qPCR experiments indicate that in humans TREK-1 is more strongly expressed in the AV node. Also species-specific differences in the cardiac electrophysiology, differential utilization of ion channels in different cardiac compartments, the vastly different heart rates and differential expression profiles of POPDC isoforms can contribute to differences in disease manifestations between mouse and man. These species-dependent differences in the phenotype already became evident when looking at the *POPDC1* and *POPDC2* null mutants that display sinus bradycardia [9] in mice, while in the zebrafish heart, which has for instance a heart rate more similar to the human heart, an AVB was observed in case of the *POPDC2* morphant in zebrafish and the *POPDC^{S191F}* mutant in mice [12,13].

It is worthwhile also to compare what is known about the clinical phenotypes associated with mutations in the other POPDC isoforms. The first reported human mutation of a *POPDC* isoform is the missense mutation *POPDC1^{S201F}* [13]. The affected patients develop AV-block and LGMD. A similar phenotype in muscle and heart is also reported for an additional three *POPDC1* mutations affecting the start codon or splicing, or resulting in a truncation of POPDC1 [14]. In contrast, in case of the *POPDC2^{W188*}* mutation, while the AV block is present, the patients do not display a LGMD phenotype. However, it is also possible that the phenotype has not yet manifested, as also in case of *POPDC1* mutations a late onset of the muscular dystrophy has been described [13]. Therefore, it can't be ruled out that a LGMD might still be developing in case of the *POPDC2^{W188*}* mutation. Recently, also the first patients carrying *POPDC3* mutations have been reported [15]. Here three different *POPDC3* mutations were discovered and homozygous patients displayed a severe LGMD, while the heart was unaffected. Clearly the three POPDC isoforms induce overlapping pathologies in striated muscles, however mutations in *POPDC2* and *POPDC3* are affecting either the heart or muscles, respectively, while *POPDC1* mutations clinically affect both muscle types. It is conceivable that this tissue-specific effects of the mutations in different *POPDC* isoforms relates to the expression levels, *POPDC2* is expressed predominantly in the heart, while *POPDC3* is preferentially expressed in skeletal muscle [7,8]. In contrast, *POPDC1* is expressed at similar levels in both striated muscle types.

The mother of the affected twins carries the $POPDC2^{W188*}$ mutation, but does not suffer from an AVB, at least until her age of 43 years. The lack or late onset of a phenotype indicates a low penetrance. The underlying mechanisms that can lead to a reduced penetrance include variations in gene expression (meaning, that there can be inter-individual variations in the gene expression levels even in members of the same family), epigenetic factors (that can be heritable changes in DNA methylation, histone modification or miRNA expression, as well as environmental and stochastic factors, which can effect gene expression levels without changing the DNA sequence), `gene-environment interplay´ (including diet, drugs, alcohol intake, metabolic syndromes and physical activity), an influence of age or sex, additional mutations or modifier genes. Thus, several of these mechanisms can be attributed for the lack of an apparent phenotype observed in the mother so far. We found that the AVB occurs in male and female patients and also at different ages, excluding sex and age as confounding factors. We do not know too much about the `gene-environment interplay´ of our patients, however, the father of the twins takes metoprolol which however should aggravate a putative AVB phenotype. We found additional putative harmful variants in *TTN* and *FKTN* in the twins presenting an AVB, but these variants were not present in the patients from the second, Italian family, here an additional putative harmful variant in *MYH7* was identified. Thus, a pure digenic inheritance that requires a second mutation in a single gene that is arrhythmogenic on its own can be excluded, giving further support to the notion that $POPDC2^{W188*}$ is the primary risk factor for the AVB. Strikingly, the additional putative disease modifying variants identified, including *TTN*, *FKT* and *MYH7*, are all associated with cardiomyopathies and muscular dystrophies. According to the concept of a mutational load, these mutations might indirectly enhance the clinical phenotype or increase AVB susceptibility caused by the $POPDC2^{W188*}$ allele. Most importantly, we observed a cardiac phenotype in mice expressing the $POPDC2^{W188*}$ mutant without the presence of additional modifiers, highlighting the pathophysiological relevance of $POPDC2^{W188*}$.

This idea of a mutational load and not a direct arrhythmogenic potential of the identified variants of *TTN*, *FKT* or *MYH7* in the different families can be derived from previous reports that associated the identical or similar variants with non-arrhythmogenic phenotypes. The identical *MYH7* variant was reported in a Moldavian family, displaying a complex phenotype characterized by Laing Distal

Myopathy-like phenotype, left ventricular non-compaction cardiomyopathy and Fiber Type Disproportion picture at muscle biopsy [28], and in another study in an Israeli Jewish family with marked lumbar lordosis, in some patients including hypertrophic cardiomyopathy [22]. Strikingly, fukutin variants were also associated with similar phenotypes, including muscular dystrophy and DCM [29]. Similarly, mutations in TTN are typically associated with dilated and other cardiomyopathies, like heart failure with preserved ejection fraction [30]. Mutations in the spring region of titin were associated with arrhythmias in the course of arrhythmogenic right ventricular dysplasia (ARVD) [20] and truncation variants in TTN were described in patients with DCM to confer a higher risk to ventricular arrhythmias [31,32]. However, the putative harmful variant that we have identified here is located in the highly conserved A-band, the most prominent region for DCM causing mutations [30,33]. Thus, as suggested by the data from the mouse model, $POPDC2^{W188*}$ is probably the primary arrhythmogenic risk factor and the additional putatively harmful variants are more likely to cause an additional pathophysiological stress to the heart.

Summarizing, our *in vivo* data give strong support to the notion that $POPDC2^{W188*}$ is a disease-related loss-of-function mutation representing a determinant factor causing the observed clinical phenotype. Therefore, *POPDC2* is a novel cardiac arrhythmia gene that along with *POPDC1* should be included as candidate gene in the genetic analysis of patients with hereditary conduction disorders.

Authors' Contributions

B.O.-B. and S.R. performed TEVC measurements and data analyses; A.K.K. and B.O.-B. performed patch clamp experiments and data analyses with HL-1 cells; S.R., B.O.-B. and A.K.K. prepared or edited all figures; B.S. analyzed WES data; C.F. and S.D. performed QPCR experiments; R.F.R.S performed site-directed mutagenesis and cell transfections for Western blot experiments; U.H.-B. helped generating and breeding the transgenic knock-in mouse line; E.S.-B., S.Z., B.S., C.R. and E.A. enrolled subjects and contributed samples and clinical data; R.S. and F.G. performed all the molecular analysis in the second family and by screening the Italian patients cohort, and A.F. supervised this work; L.Fo. and L.Fa. performed and analyzed experiments on the murine mouse model. S.R. performed the chemiluminescence assay. N.D., E.S.-B., T.B., A.F. and L.Fa. supervised the research; S.R., N.D. and

E.S.-B. acquired funding; S.R. and N.D. wrote the first draft of the manuscript and all authors contributed to the writing and editing of the revised manuscript, and approved the manuscript.

Declaration of Competing Interest

None.

References

[1]   V. Probst, F. Kyndt, F. Potet, J.N. Trochu, G. Mialet, S. Demolombe, J.J. Schott, I. Baro, D. Escande, H. Le Marec. Haploinsufficiency in combination with aging causes *SCN5A*-linked hereditary Lenegre disease. J Am Coll Cardiol 41 (2003) 643-652.

[2]   J.J. Schott, C. Alshinawi, F. Kyndt, V. Probst, T.M. Hoorntje, M. Hulsbeek, A.A. Wilde, D. Escande, M.M. Mannens, H. Le Marec. Cardiac conduction defects associate with mutations in *SCN5A*. Nat Genet 23 (1999) 20-21.

[3]   H. Watanabe, T.T. Koopmann, S. Le Scouarnec, T. Yang, C.R. Ingram, J.J. Schott, S. Demolombe, V. Probst, F. Anselme, D. Escande, A.C. Wiesfeld, A. Pfeufer, S. Kaab, H.E. Wichmann, C. Hasdemir, Y. Aizawa, A.A. Wilde, D.M. Roden, C.R. Bezzina. Sodium channel beta1 subunit mutations associated with Brugada syndrome and cardiac conduction disease in humans. J Clin Invest 118 (2008) 2260-2268.

[4]   D.W. Benson, D.W. Wang, M. Dyment, T.K. Knilans, F.A. Fish, M.J. Strieper, T.H. Rhodes, A.L. George, Jr. Congenital sick sinus syndrome caused by recessive mutations in the cardiac sodium channel gene (*SCN5A*). J Clin Invest 112 (2003) 1019-1028.

[5]   M. Kruse, E. Schulze-Bahr, V. Corfield, A. Beckmann, B. Stallmeyer, G. Kurtbay, I. Ohmert, E. Schulze-Bahr, P. Brink, O. Pongs. Impaired endocytosis of the ion channel TRPM4 is associated with human progressive familial heart block type I. J Clin Invest 119 (2009) 2737-2744.

[6]   J.P. van Tintelen, R.M. Hofstra, H. Katerberg, T. Rossenbacker, A.C. Wiesfeld, G.J. du Marchie Sarvaas, A.A. Wilde, I.M. van Langen, E.A. Nannenberg, A.J. van der Kooi, M. Kraak, I.C. van Gelder, D.J. van Veldhuisen, Y. Vos, M.P. van den Berg, l.I.C.I.o.T.N. Working Group on Inherited Cardiac Disorders. High yield of *LMNA* mutations in patients with dilated cardiomyopathy and/or conduction disease referred to cardiogenetics outpatient clinics. Am Heart J 154 (2007) 1130-1139.

[7]   B. Andree, T. Hillemann, G. Kessler-Icekson, T. Schmitt-John, H. Jockusch, H.H. Arnold, T. Brand. Isolation and characterization of the novel popeye gene family expressed in skeletal muscle and heart. Dev Biol 223 (2000) 371-382.

[8]   A. Froese, T. Brand. Expression pattern of Popdc2 during mouse embryogenesis and in the adult. Dev Dyn 237 (2008) 780-787.

[9]   A. Froese, S.S. Breher, C. Waldeyer, R.F. Schindler, V.O. Nikolaev, S. Rinné, E. Wischmeyer, J. Schlueter, J. Becher, S. Simrick, F. Vauti, J. Kuhtz, P. Meister, S. Kreissl, A. Torlopp, S.K. Liebig, S. Laakmann, T.D. Müller, J. Neumann, J. Stieber, A. Ludwig, S.K. Maier, N. Decher, H.H. Arnold, P. Kirchhof, L. Fabritz, T. Brand. Popeye domain containing proteins are essential for stress-mediated modulation of cardiac pacemaking in mice. J Clin Invest 122 (2012) 1119-1130.

[10]   S.D. Unudurthi, X. Wu, L. Qian, F. Amari, B. Onal, N. Li, M.A. Makara, S.A. Smith, J. Snyder, V.V. Fedorov, V. Coppola, M.E. Anderson, P.J. Mohler, T.J. Hund. Two-Pore K$^+$ channel TREK-1 regulates sinoatrial node membrane excitability. J Am Heart Assoc 5 (2016) e002865.

[11]   S. Simrick, R.F. Schindler, K.L. Poon, T. Brand. Popeye domain-containing proteins and stress-mediated modulation of cardiac pacemaking. Trends Cardiovasc Med 23 (2013) 257-263.

[12]   B.C. Kirchmaier, K.L. Poon, T. Schwerte, J. Huisken, C. Winkler, B. Jungblut, D.Y. Stainier, T. Brand. The Popeye domain containing 2 (popdc2) gene in zebrafish is required for heart and skeletal muscle development. Dev Biol 363 (2012) 438-450.

[13]   R.F. Schindler, C. Scotton, J. Zhang, C. Passarelli, B. Ortiz-Bonnin, S. Simrick, T. Schwerte, K.L. Poon, M. Fang, S. Rinné, A. Froese, V.O. Nikolaev, C. Grunert, T. Muller, G. Tasca, P. Sarathchandra, F. Drago, B. Dallapiccola, C. Rapezzi, E. Arbustini, F.R. Di Raimo, M. Neri, R. Selvatici, F. Gualandi, F. Fattori, A. Pietrangelo, W. Li, H. Jiang, X. Xu, E. Bertini, N. Decher, J. Wang, T. Brand, A. Ferlini. POPDC1^{S201F} causes muscular dystrophy and arrhythmia by affecting protein trafficking. J Clin Invest 126 (2016) 239-253.

[14]   W. De Ridder, I. Nelson, B. Asselbergh, B. De Paepe, M. Beuvin, R. Ben Yaou, C. Masson, A. Boland, J.F. Deleuze, T. Maisonobe, B. Eymard, S. Symoens, R. Schindler, T. Brand, K. Johnson, A. Topf, V. Straub, P. De Jonghe, J.L. De Bleecker, G. Bonne, J. Baets. Muscular dystrophy with arrhythmia caused by loss-of-function mutations in *BVES*. Neurol Genet 5 (2019) e321.

[15]   J. Vissing, K. Johnson, A. Topf, S. Nafissi, J. Diaz-Manera, V.M. French, R.F. Schindler, P. Sarathchandra, N. Lokken, S. Rinné, M. Freund, N. Decher, T. Müller, M. Duno, T. Krag, T. Brand, V. Straub. *POPDC3* gene variants associate with a new form of Limb Girdle Muscular Dystrophy. Ann Neurol 86 (2019) 832-843.

[16]   C. Friedrich, S. Rinné, S. Zumhagen, A.K. Kiper, N. Silbernagel, M.F. Netter, B. Stallmeyer, E. Schulze-Bahr, N. Decher. Gain-of-function mutation in TASK-4 channels and severe cardiac conduction disorder. EMBO Mol Med 6 (2014) 937-951.

[17]   E. Montague, L. Stanberry, R. Higdon, I. Janko, E. Lee, N. Anderson, J. Choiniere, E. Stewart, G. Yandl, W. Broomall, N. Kolker, E. Kolker. MOPED 2.5--an integrated multi-omics resource: multi-omics profiling expression database now includes transcriptomics data. OMICS 18 (2014) 335-343.

[18]   K.R. Thomas, M.R. Capecchi. Site-directed mutagenesis by gene targeting in mouse embryo-derived stem cells. Cell 51 (1987) 503-512.

[19]   H.S. Nam, R. Benezra. High levels of Id1 expression define B1 type adult neural stem cells. Cell Stem Cell 5 (2009) 515-526.

[20]   M. Taylor, S. Graw, G. Sinagra, C. Barnes, D. Slavov, F. Brun, B. Pinamonti, E.E. Salcedo, W. Sauer, S. Pyxaras, B. Anderson, B. Simon, J. Bogomolovas, S. Labeit, H. Granzier, L. Mestroni.

Genetic variation in titin in arrhythmogenic right ventricular cardiomyopathy-overlap syndromes. Circulation 124 (2011) 876-885.

[21] F. Brun, C.V. Barnes, G. Sinagra, D. Slavov, G. Barbati, X. Zhu, S.L. Graw, A. Spezzacatene, B. Pinamonti, M. Merlo, E.E. Salcedo, W.H. Sauer, M.R. Taylor, L. Mestroni, R. Familial Cardiomyopathy. Titin and desmosomal genes in the natural history of arrhythmogenic right ventricular cardiomyopathy. J Med Genet 51 (2014) 669-676.

[22] P.J. Lamont, W. Wallefeld, D. Hilton-Jones, B. Udd, Z. Argov, A.C. Barboi, C. Bonneman, K.M. Boycott, K. Bushby, A.M. Connolly, N. Davies, A.H. Beggs, G.F. Cox, J. Dastgir, E.T. DeChene, R. Gooding, H. Jungbluth, N. Muelas, J. Palmio, S. Penttila, E. Schmedding, T. Suominen, V. Straub, C. Staples, P.Y. Van den Bergh, J.J. Vilchez, K.R. Wagner, P.G. Wheeler, E. Wraige, N.G. Laing. Novel mutations widen the phenotypic spectrum of slow skeletal/beta-cardiac myosin (*MYH7*) distal myopathy. Hum Mutat 35 (2014) 868-879.

[23] E. Pegoraro, B.F. Gavassini, C. Borsato, P. Melacini, A. Vianello, R. Stramare, G. Cenacchi, C. Angelini. *MYH7* gene mutation in myosin storage myopathy and scapulo-peroneal myopathy. Neuromuscul Disord 17 (2007) 321-329.

[24] C. Di Resta, A. Pietrelli, S. Sala, P. Della Bella, G. De Bellis, M. Ferrari, R. Bordoni, S. Benedetti. High-throughput genetic characterization of a cohort of Brugada syndrome patients. Hum Mol Genet 24 (2015) 5828-5835.

[25] M.R. Hazebroek, S. Moors, R. Dennert, A. van den Wijngaard, I. Krapels, M. Hoos, J. Verdonschot, J.J. Merken, B. de Vries, P.F. Wolffs, H.J. Crijns, H.P. Brunner-La Rocca, S. Heymans. Prognostic relevance of gene-environment interactions in patients with dilated cardiomyopathy: applying the MOGE(S) classification. J Am Coll Cardiol 66 (2015) 1313-1323.

[26] W.C. Claycomb, N.A. Lanson, Jr., B.S. Stallworth, D.B. Egeland, J.B. Delcarpio, A. Bahinski, N.J. Izzo, Jr. HL-1 cells: a cardiac muscle cell line that contracts and retains phenotypic characteristics of the adult cardiomyocyte. Proc Natl Acad Sci U.S.A. 95 (1998) 2979-2984.

[27] X. Wang, N.R. Tucker, G. Rizki, R. Mills, P.H. Krijger, E. de Wit, V. Subramanian, E. Bartell, X.X. Nguyen, J. Ye, J. Leyton-Mange, E.V. Dolmatova, P. van der Harst, W. de Laat, P.T. Ellinor, C. Newton-Cheh, D.J. Milan, M. Kellis, L.A. Boyer. Discovery and validation of sub-threshold genome-wide association study loci using epigenomic signatures. Elife 5 (2016)

[28] L. Ruggiero, C. Fiorillo, S. Gibertini, F. De Stefano, F. Manganelli, R. Iodice, F. Vitale, S. Zanotti, M. Galderisi, M. Mora, L. Santoro. A rare mutation in *MYH7* gene occurs with overlapping phenotype. Biochem Biophys Res Commun 457 (2015) 262-266.

[29] T. Murakami, Y.K. Hayashi, S. Noguchi, M. Ogawa, I. Nonaka, Y. Tanabe, M. Ogino, F. Takada, M. Eriguchi, N. Kotooka, K.P. Campbell, M. Osawa, I. Nishino. Fukutin gene mutations cause dilated cardiomyopathy with minimal muscle weakness. Ann Neurol 60 (2006) 597-602.

[30]   M.M. LeWinter, H.L. Granzier. Titin is a major human disease gene. Circulation 127 (2013) 938-944.

[31]   B. Corden, J. Jarman, N. Whiffin, U. Tayal, R. Buchan, J. Sehmi, A. Harper, W. Midwinter, K. Lascelles, V. Markides, M. Mason, J. Baksi, A. Pantazis, D.J. Pennell, P.J. Barton, S.K. Prasad, T. Wong, S.A. Cook, J.S. Ware. Association of titin-truncating genetic variants with life-threatening cardiac arrhythmias in patients with dilated cardiomyopathy and implanted defibrillators. JAMA Netw Open 2 (2019) e196520.

[32]   J.A.J. Verdonschot, M.R. Hazebroek, K.W.J. Derks, A. Barandiaran Aizpurua, J.J. Merken, P. Wang, J. Bierau, A. van den Wijngaard, S.M. Schalla, M.A. Abdul Hamid, M. van Bilsen, V.P.M. van Empel, C. Knackstedt, H.P. Brunner-La Rocca, H.G. Brunner, I.P.C. Krapels, S.R.B. Heymans. Titin cardiomyopathy leads to altered mitochondrial energetics, increased fibrosis and long-term life-threatening arrhythmias. Eur Heart J 39 (2018) 864-873.

[33]   D.S. Herman, L. Lam, M.R. Taylor, L. Wang, P. Teekakirikul, D. Christodoulou, L. Conner, S.R. DePalma, B. McDonough, E. Sparks, D.L. Teodorescu, A.L. Cirino, N.R. Banner, D.J. Pennell, S. Graw, M. Merlo, A. Di Lenarda, G. Sinagra, J.M. Bos, M.J. Ackerman, R.N. Mitchell, C.E. Murry, N.K. Lakdawala, C.Y. Ho, P.J. Barton, S.A. Cook, L. Mestroni, J.G. Seidman, C.E. Seidman. Truncations of titin causing dilated cardiomyopathy. N Engl J Med 366 (2012) 619-628.